EuroIntervention 2013;8:1441-1450

Bioresorbable drug-eluting magnesium-alloy scaffold: design and feasibility in a porcine coronary model

Eric Wittchow[1]*, PhD; Nina Adden[1], PhD; Johannes Riedmüller[1]; Claudine Savard[2], DVM, MSC; Ron Waksman[3], MD; Marlen Braune[1], PhD

1. Biotronik SE & Co. KG, Erlangen, Germany; 2. AccelLAB Inc., Boisbriand, Canada; 3. Washington Hospital Center, Washington, USA

KEYWORDS

- bioresorbable PLGA polymer
- bioresorbable scaffold
- drug-eluting stent
- magnesium scaffold degradation products
- paclitaxel
- porcine coronary model

Abstract

Aims: Among three versions of bioresorbable magnesium scaffolds featuring different paclitaxel-elution kinetics, we determined the best-performing scaffold and compared it with established, paclitaxel-eluting, permanent stents TAXUS Liberté and eucaTAX.

Methods and results: Drug-elution kinetics in magnesium scaffolds were modulated by varying the composition of their bioresorbable poly(lactide-*co*-glycolide) coating loaded with paclitaxel. A 50:50 ratio of lactide to glycolide, or an 85:15 ratio and either high- or low-molecular-weight polymer was applied in the "50/50", "85/15H", and "85/15L" scaffolds, respectively. Seventy-three magnesium scaffolds (25 50/50, 24 85/15H, 24 85/15L) and 36 control stents (18 TAXUS Liberté, 18 eucaTAX) were implanted in coronary arteries of 50 Yucatan mini-pigs. Angiography, histomorphometry, and histopathology data were acquired at 28, 90 and 180 days. The best-performing magnesium scaffold, 85/15H, was equivalent to TAXUS Liberté and superior to eucaTAX regarding late luminal loss, intimal area, fibrin score, and endothelialisation. Intimal inflammation score was higher in 85/15H than in the control stents at 28 days, but this effect disappeared at later time points.

Conclusions: By selecting suitable paclitaxel-elution kinetics, it was feasible to develop a bioresorbable magnesium scaffold whose efficacy and healing characteristics in a porcine coronary model are comparable with those of established paclitaxel-eluting permanent metallic stents.

**Corresponding author: BIOTRONIK SE & Co. KG, Hartmannstr. 65, 91052 Erlangen, Germany. E-mail: eric.wittchow@biotronik.com*

DOI: 10.4244/EIJV8I12A218

Introduction

Bioresorbable scaffolds offer numerous potential advantages over current stent technologies and are therefore heralded as the fourth revolution in interventional cardiology after the invention of balloon angioplasty, bare metal stents, and drug-eluting stents[1-3]. The major putative advantages of bioresorbable scaffolds are a lower risk of late stent thrombosis and a reduced requirement for long-term dual antiplatelet therapy upon complete resorption, because no triggers for thrombosis such as uncovered stent struts, durable polymer, or remnant drug should remain[1,2]. The absence of a rigid metallic cage can facilitate not only the restoration of the vessel vasomotor tone, but also adaptive shear stress, late luminal enlargement, and late expansive remodelling[2]. This entire process, rendering the vessel fully amenable to biological, pharmacological, and physiological impact, has recently been named vascular reparative therapy[2].

Animal and human studies have shown that magnesium (Mg) alloys can be safely used in bioresorbable scaffolds[1,4-8]. The first generation of bioresorbable metal scaffolds (AMS-1; Biotronik AG, Bülach, Switzerland) was made from a WE43 alloy, composed of 93% Mg and 7% rare earth elements. After deployment in porcine coronary arteries, the AMS-1 scaffold was rapidly endothelialised and largely degraded into inorganic ions within 60 days, with little associated inflammatory response[5]. In humans, AMS-1 was implanted both in coronary and peripheral vessels[7-16]. No safety concerns were raised regarding deaths, myocardial infarction, or stent thrombosis[7]. However, the long-term patency rates were lower than expected[7,14-16]. The primary mechanism of restenosis appeared to be vessel recoil after early loss of radial force due to scaffold degradation, seemingly progressing faster than anticipated[1,7,15,17]. Moreover, intra- and extra-scaffold neointima formation was observed[1,7,15].

To prolong vessel scaffolding and reduce neointimal growth, AMS-1 was redesigned and coated with a bioresorbable poly(lactide-*co*-glycolide) polymer matrix (PLGA)[3,18] containing the antiproliferative drug paclitaxel[19-21]. Paclitaxel release kinetics can vary largely with PLGA composition[22], and the ideal kinetics have yet to be found. To this end, the aims of the present study were: (1) to identify the optimal of three PLGA compositions applied alternately as drug carriers in the novel AMS-3.0 scaffold; and (2) to compare the safety and efficacy of the best AMS-3.0 option with two established, paclitaxel-eluting, permanent stents used as controls. One control stent was selected to have permanent polymer coating as drug carrier (TAXUS® Liberté®; Boston Scientific, Natick, MA, USA)[20], and the other control stent (eucaTAX; eucatech AG, Rheinfelden, Germany)[23] had, like AMS-3.0, a PLGA coating whose degradation products could influence inflammation scores by attracting macrophages.

Methods

The comparisons were based on angiography, histomorphometry, and histopathology data acquired in a porcine coronary artery model at 28, 90 and 180 days. The study protocol was approved by the Institutional Animal Care and Use Committee of the testing facility (AccelLAB Inc., Boisbriand, Quebec, Canada) and was in compliance with the Canadian Council on Animal Care regulations.

AMS-3.0 SCAFFOLD

The balloon-expandable AMS-3.0 scaffold (Biotronik AG, Bülach, Switzerland) uses a refined, slower-degradable WE43 alloy and has a higher collapse pressure than AMS-1 (1.5 vs. 0.8 bar). To preserve radial strength during anisotropic scaffold degradation in a biological environment over a longer time period, the cross-sectional profile of scaffold struts in AMS-3.0 was redesigned to be square-shaped, as opposed to the rectangular shape in AMS-1 **(Figure 1)**. Thereby, strut thickness was reduced from 165 to 120 µm, which should facilitate endothelialisation and reduce restenosis[3,24-26].

The degradation rate of the drug-carrying PLGA polymer, and hence the paclitaxel release rate, is mandated by the modifiable lactide to glycolide ratio[18]. A 50:50 ratio speeds up PLGA degradation, and a discrepant ratio of lactide to glycolide (in whichever direction) slows it down[18]. The present study tested three versions of AMS-3.0 scaffolds differing in their PLGA composition **(Table 1)**.

CONTROL STENTS

Both control stents, TAXUS Liberté and eucaTAX, were balloon-expandable, paclitaxel-eluting, 16 mm x 3.0 mm devices. Both had a non-degradable stainless steel platform with a strut thickness of 97 µm (TAXUS Liberté) or 85 µm (eucaTAX). The metallic platform in TAXUS Liberté was coated with 18 µm thick permanent polymer poly(styrene-isobutylene-styrene) containing 108 µg of paclitaxel[19,20]. In eucaTAX, the metallic platform was coated with 100 nm glycocalyx[23,27] and 3-5 µm thick PLGA loaded with 25 µg

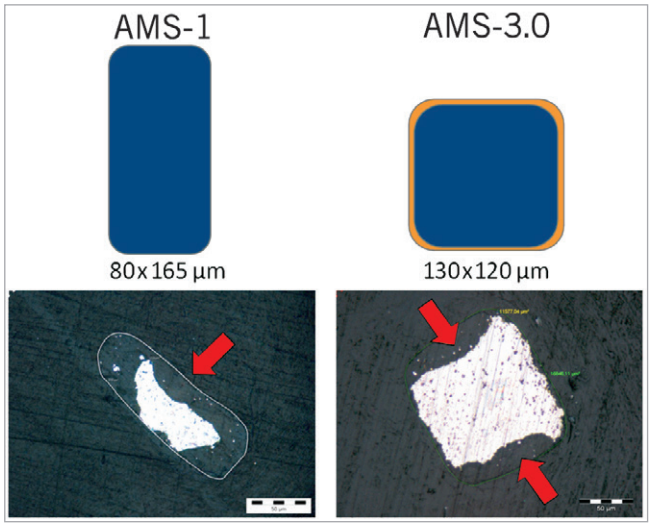

Figure 1. *Schematic cross-sectional profile of scaffold struts in AMS-1 and AMS-3.0 (top) and the appearance of struts under the light microscope (unstained ground sections) 28 days after implantation in a porcine coronary model (bottom, archive data). By scaffold degradation in vivo, a preferential attack occurs at the lateral sides (denoted by arrows), which are intensely colonised by cells (e.g., macrophages) because of fluid flow phenomena. The poly(lactide-co-glycolide)-coating of the AMS-3.0 scaffold is indicated by the thin orange layer. AMS-1: the first-generation absorbable metal scaffold; AMS-3.0: the third-generation absorbable metal scaffold.*

Table 1. Scaffolds and stents compared in this study.

Device model	Lactide to glycolide ratio in PLGA	Molecular weight of PLGA	PLGA thickness	Paclitaxel amount
AMS-3.0 scaffolds				
85/15H	85:15	high	1 µm	8 µg
85/15L	85:15	low	1 µm	8 µg
50/50	50:50	high	3 µm	10 µg
Control stents				
TAXUS Liberté	N.A.*	N.A.	N.A.*	108 µg
eucaTAX	50:50	high	3-5 µm	25 µg

The three AMS-3.0 scaffolds were otherwise identical (16 mm x 3.0 mm), with a strut geometry depicted in Figure 1. *18 µm thick poly(styrene-isobutylene-styrene) used instead of PLGA. AMS-3.0: the third-generation absorbable metal scaffold; N.A.: not applicable; PLGA: poly(lactide-*co*-glycolide) matrix coating the scaffold and carrying the paclitaxel

of paclitaxel[23]. TAXUS has been studied extensively since 2003[20,21], while eucaTAX is a newer stent that received the European Conformity mark (CE mark) in 2007[23].

ANIMALS, ANAESTHESIA, AND MEDICATION

Fifty Yucatan mini-pigs (19 females and 31 castrated males), weighing 39-58 kg, were allocated to the 28-day (n=19), 90-day (n=17), and 180-day (n=14) cohorts. Anaesthesia was induced by an intravenous propofol injection. The animals were intubated and supported by mechanical ventilation. Isoflurane in oxygen was administered to maintain a surgical plane of anaesthesia. Bupivacaine was given intramuscularly to achieve local anaesthesia and, combined with butorphanol, to manage pain after surgery. The antithrombotic regimen consisted of an intravenous heparin bolus of ~400 U/kg given before catheterisation, followed by additional heparin administration whenever the activated clotting time, measured every 30 minutes or less, fell below 300 seconds. Acetylsalicylic acid (325 mg/day) and clopidogrel (300 mg on the first day and 75 mg/day thereafter) were started ≥3 days before angioplasty and continued until sacrifice.

IMPLANTATION PROCEDURE

After insertion of the guiding catheter, nitroglycerine was injected intracoronarily to induce vasodilation. Segments of the left anterior descending artery, left circumflex artery, and right coronary artery with favourable anatomy and diameter (~2.5 mm) were selected by coronary angiography and assigned to different scaffold or stent models using a table predefined in the study protocol. The devices were implanted using a balloon pressure targeting 20% overdilation. No more than one device was positioned in a single artery. After post-treatment recovery, the animals were returned to care facilities, where they received a normal diet.

QUANTITATIVE CORONARY ANGIOGRAPHY

In each animal, quantitative coronary angiography (QCA) was performed before the treatment, at full balloon inflation, after the treatment, and before euthanasia. In addition, an intermediate angiogram was taken at 60 days in the 90-day cohort and at 135 days in the 180-day cohort. For each recording, a single image of the treated area was selected and the QCA analysis was performed using Medis QCA-CMS 6.0 software (Medis, Leiden, The Netherlands). The parameters measured were balloon to artery ratio (oversize) and late luminal loss. To increase the reproducibility of late luminal loss assessments, the post-treatment and all later angiograms were taken at two orthogonal angles and the mean values were calculated.

HISTOMORPHOMETRY AND HISTOPATHOLOGY

Harvested hearts were perfusion-rinsed with lactated Ringer's solution and fixated by pressure perfusion (100 ml/min) and immersion using neutral buffered formalin. The treated vessel segment was removed in a block with adjacent tissues, dehydrated, and embedded in methyl methacrylate. The stented or scaffolded artery part was divided into three similarly long segments (proximal, middle, distal). Histological sections (~8 µm thick) were obtained from each segment and stained with haematoxylin-eosin and Verhoeff-van Giesen for light microscopy with image capture.

Computer-assisted morphometry was performed to determine intimal area (a difference between the area within the internal elastic lamina and the luminal area) and medial area (the area between external and internal elastic laminae). The calculations were made using Image Pro Plus 6.1.0.346 (Media Cybernetics Inc., Silver Spring, MD, USA) software.

Semi-quantitative and descriptive histopathology included scores for inflammation, intimal fibrin content, and endothelialisation. Each scaffold or stent strut in a cross-section was graded as: 0=no or very few (≤3) inflammatory cells around the strut; 1=few (~4-10) inflammatory cells around the strut; 2=many (>10) inflammatory cells around the strut that can extend into, but do not efface, surrounding tissue; or 3=many (>10) inflammatory cells, effacing the surrounding tissue architecture. The mean inflammation score for the cross-section was then calculated as the sum of grades for each strut divided by the number of struts present. The inflammation score for the scaffold or stent was determined as the mean of the cross-section scores.

An analogous calculation principle was used for the intimal fibrin content score, whereby a strut was graded as: 0=no fibrin, or rare minimal spotting around the strut; 1=small amount of fibrin localised only around the strut; 2=moderately abundant or denser fibrin extending beyond the strut; or 3=abundant and dense fibrin bridging between struts. The endothelialisation score was derived for each cross-section by the portion of artery circumference covered by endothelium: 0=<25% covered, 1=25-75% covered, 2=76-99% covered, or 3=100% covered. The mean of the cross-section scores represented the endothelialisation score for the scaffold or stent.

The AMS-3.0 degradation products at 28, 90 and 180 days were characterised by energy-dispersive X-ray spectroscopy using a Zeiss EVO 15 LS scanning electron microscope (Carl Zeiss Microimaging GmbH, Göttingen, Germany). The images were analysed with Bruker-Esprit 1.8 software (Bruker AXS GmbH, Karlsruhe, Germany), with standard mapping option applied.

DRUG-ELUTION KINETICS TEST

Aiming to elucidate the role of different polymer coatings as drug carriers, we compared *in vitro* the drug-elution kinetics for the three AMS-3.0 versions, TAXUS Liberté, and eucaTAX. For this test, the bioresorbable Mg-alloy platform in AMS-3.0 was replaced with a permanent stainless steel (316L) platform to eliminate the influence of unnatural scaffold fragmentation *in vitro*.

STATISTICAL METHODS

Continuous variables are presented as mean ± SD unless stated otherwise. The data were checked for normal distribution by the Kolmogorov-Smirnov test and the Levene median test for equal variances. For multiple comparisons, analysis of variance (ANOVA; with Tukey *post hoc* comparisons) or the Kruskal-Wallis test (ranks with Dunn's method pairwise) were used as appropriate. A p-value <0.05 was considered statistically significant.

Results

IMPLANTATION AND FOLLOW-UP

A total of 109 scaffolds or stents were implanted in the 28-day (n=36), 90-day (n=36), and 180-day (n=37) study cohorts. The nearly identical distribution of different devices across study cohorts and a fairly balanced use of the three coronary arteries are shown in **Table 2**. The mean balloon to artery ratio (oversize) ranged from 1.19±0.04 to 1.27±0.07, with no significant difference between the 15 groups (5 devices x 3 study cohorts).

No animal died before scheduled euthanasia. Neither QCA nor histological studies revealed thrombosis, aneurysm-like vessel widening or any other severe adverse effect in any pig studied.

COMPARISON OF THREE AMS-3.0 VERSIONS

The 50/50 version was associated with the largest intimal area, highest fibrin content score, and lowest endothelialisation score at 28 days, and with the largest late luminal loss at 60-180 days **(Figure 2)**. The differences between the other two AMS-3.0 versions, 85/15H and 85/15L, were not significant for any parameter, but 85/15H showed a tendency for less intimal area at 28 days and 180 days, and for a higher endothelialisation score at 28 days. We considered, therefore, 85/15H to be the best-performing AMS-3.0 version, with a slight advantage over 85/15L.

Table 2. Distribution of implanted devices across coronary arteries and study cohorts.

Device model	Number of devices for 28d/90d/180d (Total)			
	LAD	LCX	RCA	Total
AMS-3.0 scaffolds				
85/15H	3/2/3 (8)	1/2/2 (5)	4/4/3 (11)	8/8/8 (24)
85/15L	2/3/3 (8)	2/3/2 (7)	4/2/3 (9)	8/8/8 (24)
50/50	2/3/3 (8)	2/2/2 (6)	4/3/4 (11)	8/8/9 (25)
Control stents				
TAXUS Liberté	3/3/2 (8)	1/1/2 (4)	2/2/2 (6)	6/6/6 (18)
eucaTAX	2/2/2 (6)	2/2/2 (6)	2/2/2 (6)	6/6/6 (18)
Total devices	12/13/13 (38)	8/10/10 (28)	16/13/14 (43)	36/36/37 (109)

28d/90d/180d: 28-day, 90-day, and 180-day study cohorts; AMS-3.0 scaffolds are defined in Table 1; LAD: left anterior descending artery; LCX: left circumflex artery; RCA: right coronary artery

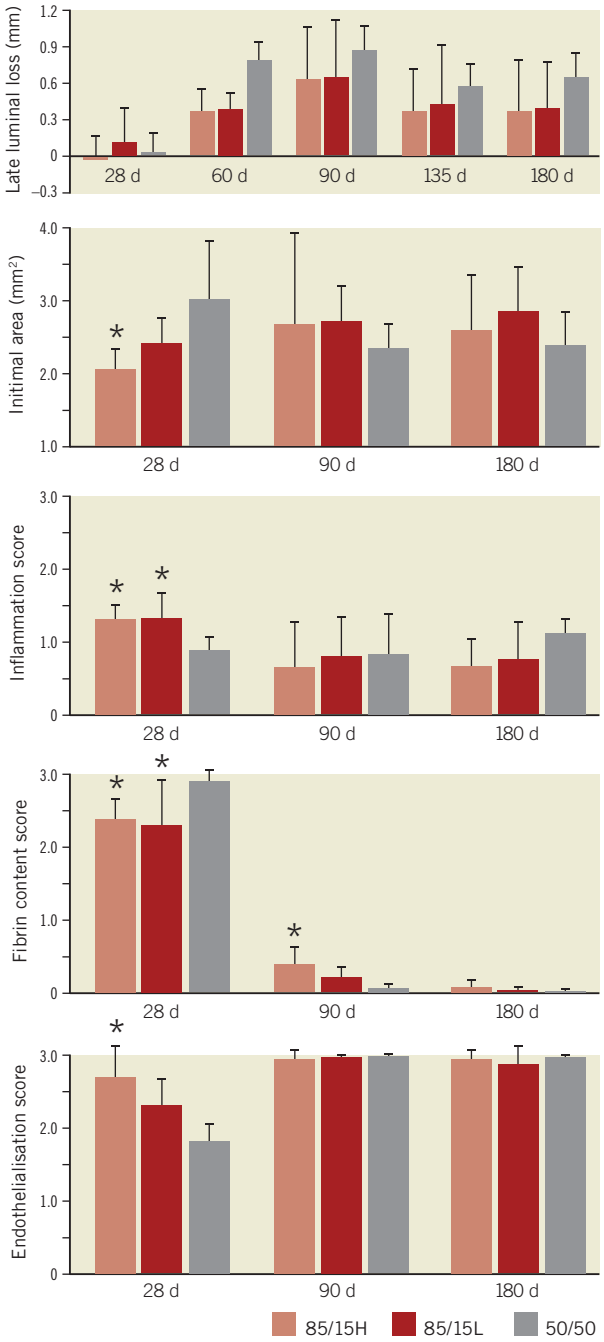

Figure 2. *Comparisons of late luminal loss (determined by QCA), intimal area (histomorphometry), inflammation scores, intimal fibrin content, and endothelialisation scores (histopathology) for the three AMS-3.0 versions defined in Table 1. Mean values and standard deviations are shown. *p<0.05 versus 50/50. There were no statistically significant differences between 85/15H and 85/15L. The number of scaffolds per version and follow-up point was 8, except for 9 50/50 scaffolds at 135 and 180 days. QCA: quantitative coronary angiography*

COMPARISON OF 85/15H AND CONTROL STENTS

For late luminal loss, the 85/15H scaffold was similar to TAXUS Liberté during the entire observational period and better than eucaTAX at 60-180 days **(Figure 3)**. Moreover, the mean intimal area for 85/15H was always slightly smaller than that for TAXUS Liberté and substantially smaller than that for eucaTAX. Although the intimal inflammation score was higher in 85/15H than in the control stents at 28 days, no important differences were seen at later time points. Conversely, 85/15H had advantages over TAXUS Liberté and especially over eucaTAX for fibrin score and endothelialisation score at 28 days, but no differences were seen at later time points **(Figure 3)**. The values are tabulated in **Table 3**, which also compares medial areas and the inflammation scores for media and adventitia.

HISTOLOGICAL IMAGES

Representative histological sections for 85/15H, TAXUS Liberté, and eucaTAX, taken at 28-180 days, are presented in **Figure 4**. High-power histological images taken at 28 days for all five devices studied are shown in **Figure 5**.

Table 3. Comparison of 85/15H, TAXUS Liberté, and eucaTAX.

Variable		85/15H	TAXUS Liberté	eucaTAX
Late luminal loss (mm)	28 days	–0.03±0.17	–0.03±0.18	–0.10±0.19
	60 days	0.36±0.20	0.46±0.16	0.84±0.22
	90 days	0.65±0.41	0.56±0.33*	1.08±0.23
	135 days	0.37±0.36*	0.37±0.35*	0.93±0.29
	180 days	0.37±0.42	0.45±0.35	0.82±0.28
Intimal area (mm^2)	28 days	2.06±0.28*	2.53±0.51	2.89±0.36
	90 days	2.68±1.26	2.92±1.08	3.63±0.42
	180 days	2.60±0.76*	2.74±1.04	3.77±0.57
Medial area (mm^2)	28 days	1.13±0.18	1.25±0.17	1.29±0.25
	90 days	0.67±0.18¶	1.03±0.34*	0.57±0.16
	180 days	0.94±0.31	1.32±0.50*	0.46±0.18
Intimal inflammation score	28 days	1.31±0.20*¶	0.56±0.15	0.48±0.22
	90 days	0.65±0.65	0.70±0.22	0.19±0.15
	180 days	0.66±0.39	0.38±0.26	0.34±0.29
Intimal fibrin content score	28 days	2.35±0.28*	2.68±0.22	2.97±0.04
	90 days	0.37±0.24	0.50±0.40	0.09±0.03
	180 days	0.07±0.09	0.27±0.35	0.02±0.04
Endothelialisation score	28 days	2.71±0.42*	2.39±0.49	1.22±0.50
	90 days	2.96±0.12	2.89±0.17	3.00±0.00
	180 days	2.96±0.12	3.00±0.00	3.00±0.00
Medial inflammation score	28 days	1.29±0.55¶	0.33±0.42	0.67±0.42
	90 days	0.33±0.50	0.61±0.68	0.28±0.33
	180 days	0.38±0.42	0.17±0.28	0.22±0.27
Adventitial inflammation score	28 days	0.88±0.47*¶	0	0.06±0.13
	90 days	0.42±0.73	0.33±0.56	0.22±0.40
	180 days	0.25±0.34	0.11±0.17	0.28±0.68

Data are presented as mean±SD. *$p<0.05$ vs. eucaTAX; ¶$p<0.05$ vs. TAXUS Liberté. The numbers of scaffolds and stents as in Figure 3.

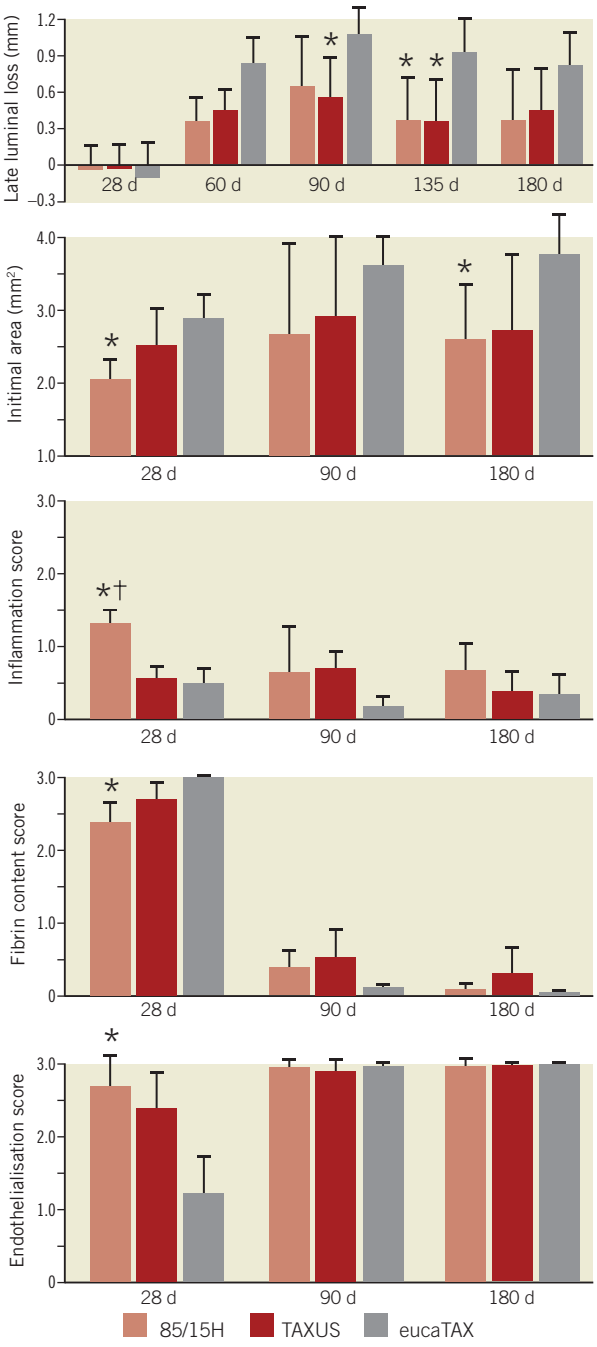

Figure 3. *Comparison of 85/15H (the best scaffold in Figure 2) and TAXUS Liberté and eucaTAX stents. Mean values and standard deviations are shown. *$p<0.05$ versus eucaTAX. †$p<0.05$ versus TAXUS Liberté. The number of scaffolds at each follow-up point was 8 for 85/15H, 6 for TAXUS Liberté, and 6 for eucaTAX.*

The dynamics and products of 85/15H degradation at 28 days, 90 days and 180 days are described in **Figure 6**. Mg-alloy is not decayed completely, but converted into a soft and gel-like amorphous degradation product. Although the exact chemical degradation process is still subject to research, roughly two phases can be differentiated. First, an Mg-rich compound containing a large amount of oxygen is formed, possibly representing a mixture of Mg hydroxide

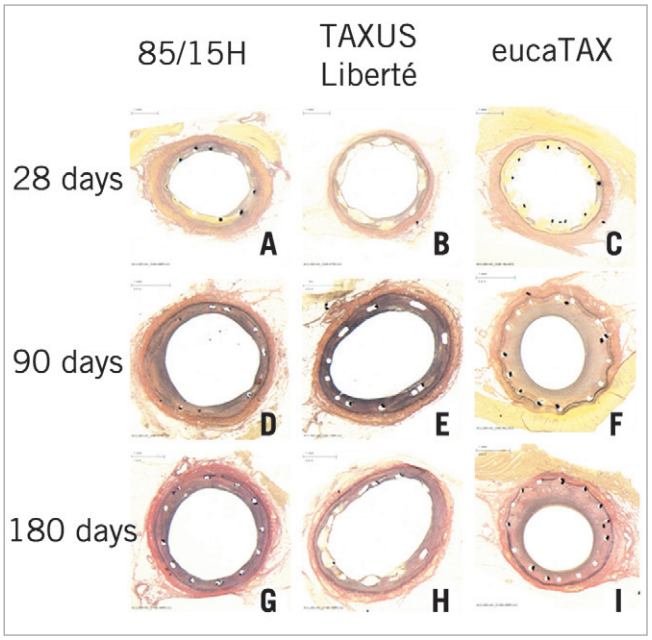

Figure 4. *Representative histological sections removed at 28 days (A-C), 90 days (D-F), and 180 days (G-I) and stained with Verhoeff-van Giesen. Note small or even absent media in panels F, G and I.*

and Mg carbonate. Several weeks later, these compounds convert to amorphous calcium phosphate, taking exactly the morphology of the dissolved scaffold struts. Measured at 28 days, the average *in vivo* degradation rates for the three AMS-3.0 versions ranged from 0.036-0.072 mg/(cm^2*day).

DRUG-ELUTION KINETICS *IN VITRO*

EucaTAX delivered the highest daily drug doses, resulting in complete paclitaxel elution within eight weeks. TAXUS Liberté released paclitaxel according to a biphasic elution profile, that is, intensively within the first two days and slowly thereafter. Despite using degradable PLGA polymer as drug carrier, both 85/15H and 85/15L exhibited slow and long-lasting elution kinetics similar to that for TAXUS Liberté **(Figure 7)**.

Discussion

The present study shows that a drug-eluting absorbable metal scaffold can effectively prevent late luminal loss in the porcine coronary model, with relative safety, as demonstrated in preclinical studies[28], similar to that of TAXUS Liberté. At 28 days, traditionally the most relevant follow-up point in porcine studies, the late luminal loss assessed by QCA was negligible for all devices studied. This is probably attributable to the strong cell growth inhibitory effect of paclitaxel[20], levelling different drug-eluting stent concepts at this point. Thereafter, an accentuated late luminal loss had occurred sooner (at 60 days) in the devices with short drug-elution periods, eucaTAX and 50/50, than in the devices with longer drug-elution periods: 85/15H, 85/15L, and TAXUS Liberté (at 90 days).

Considering the different timescales for healing of human and porcine coronary arteries[18,29,30], the better preclinical efficacy at 90 days is in general well transferred into the better angiographic outcome at ≥9 months. The lower late luminal loss for TAXUS Liberté than for eucaTAX at 90 days in the present study is, thus, in line with the lower late luminal loss in the TAXUS ATLAS[31] clinical trial (0.42±0.54 mm, at 9 months) compared with the EUCATAX[23] trial: 0.52±0.59 mm, at 12 months. Hence, the similar late luminal loss for 85/15H and for TAXUS Liberté at 90 days **(Figure 3)** implies that their clinical efficacy at ≥9 months is probably similar.

The notion of Jabara et al[18] that longer-lasting, effective drug elution postpones if not suppresses the aggressive neointimal growth is corroborated by our results for different AMS-3.0 versions. This postponement, however, does not necessarily correspond to the drug-elution period. Thus, in TAXUS Liberté, paclitaxel elution probably continues beyond 180 days, while the neointimal growth in the porcine coronary model appears to reach its maximum at ~90 days and declines thereafter. This resorptive phase of the intima during maturation, reflected through a slight to moderate decrease of intimal area, is also known from bare metal stents, where aggressive neointimal formation occurs earlier[18].

The observed discrepancy between a minor late luminal loss and a large neointimal area for both eucaTAX and 50/50 at 28 days might have been caused by the QCA's inability to identify luminal reduction

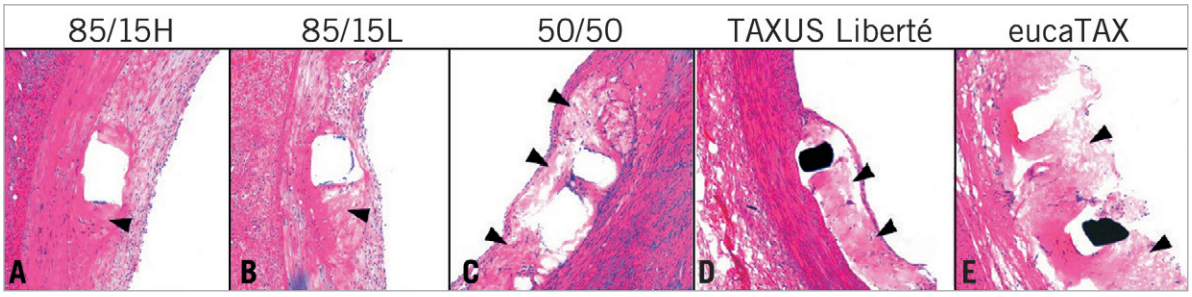

Figure 5. *Representative high-power images of histological sections removed at 28 days and stained with haematoxylin-eosin. Presence of fibrin deposition (black arrowheads) depends on polymer composition and more fibrin was seen in the fast-degrading 50/50, because of fast drug elution and polymer degradation, than in the slow-degrading 85/15H. High daily drug dose in eucaTAX delayed healing and tissue coverage compared with TAXUS Liberté. The consistently low inflammation scores for eucaTAX were seemingly caused by the lack of tissue since high daily doses of paclitaxel can elicit a profound cell toxic response.*

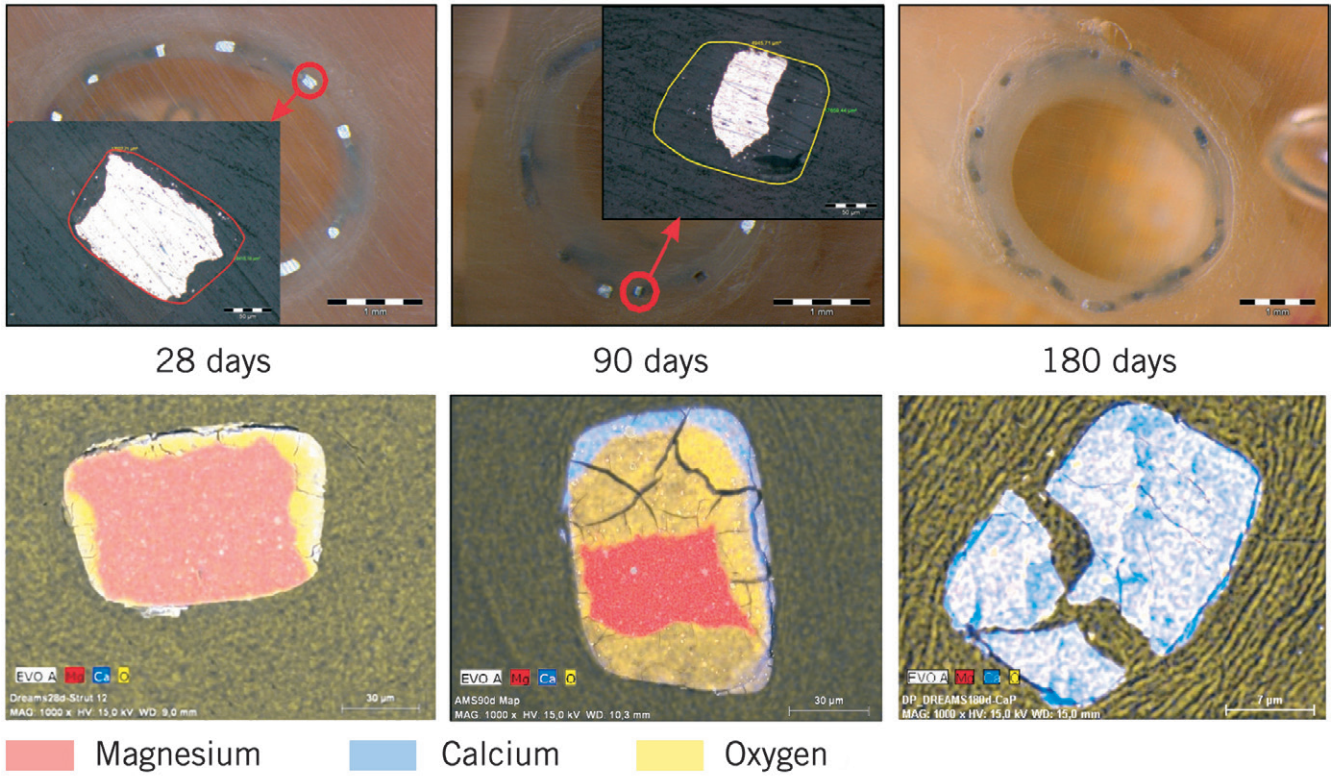

Figure 6. *Scanning electron microscope images (upper panels) and energy-dispersive X-ray mapping of AMS-3.0 degradation products (lower panels, unrelated to upper panels). At 28 days, non-degraded magnesium-alloy particles had been surrounded by magnesium, calcium, and oxygen, probably in the form of $MgCO_3$ or $Mg(OH)_2$ or both, which could not be differentiated without further analysis. At 90 days, magnesium-alloy area was reduced, while oxidated (yellow) areas had become partly replaced at their outer margins by a calcium-phosphorous-oxygen compound (blueish area). Raman and infrared spectroscopy combined with X-ray defraction analysis clarified that this was calcium phosphate with amorphous structure. At 180 days, no remaining metallic particles were noted.*

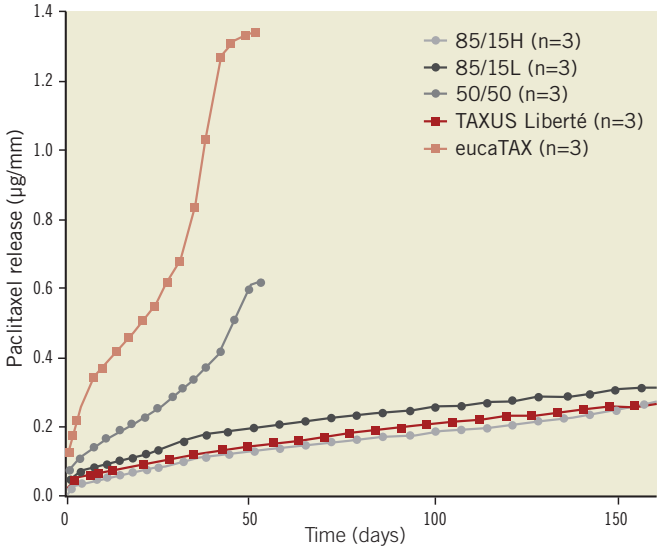

Figure 7. *Comparison of paclitaxel-elution kinetics in vitro. Results are presented as mean ± SD. For this test, the degradable magnesium-alloy platform in AMS-3.0 scaffolds was replaced with a non-degradable stainless steel platform.*

caused by fibrin, while per definition all fibrin depositions contributed to neointima within the histomorphometric evaluations. The higher fibrin scores for eucaTAX and 50/50 than for other devices at 28 days were a likely consequence of the faster drug elution with eucaTAX and 50/50. At 90 days, all fibrin scores had reduced substantially but reached 0 seemingly only if paclitaxel release had ceased completely. The endothelialisation scores were inversely correlated to fibrin scores. Endothelialisation was nearly completed within 90 days in all devices.

Although the inflammation scores were generally low, the difference between 85/15H and the control stents reached statistical significance at 28 days. This was presumably caused by macrophage activity triggered by scaffold degradation products. At 90 days, the inflammation for 85/15H had subsided to the level observed for control stents. Of note, the low inflammation score for eucaTAX at 28 days was most likely caused by a reduced number of cells in the surrounding tissue, since high daily doses of paclitaxel can elicit a profound toxic response[18].

SCAFFOLD DEGRADATION

While degradation *in vitro* progresses equally from all sides, *in vivo* a preferential attack occurs at the lateral sides, which are intensely

colonised by cells because of fluid flow phenomena[26]. In particular, the macrophages have the ability to attack polymers and alloys by releasing acid digestion cocktails[32]. Since this complex interplay is difficult to mimic *in vitro,* major differences between *in vitro* and *in vivo* decomposition of degradable materials can be seen in conditions when macrophages play a role in the biological environment[33]. We compared the *in vivo* AMS-3.0 degradation rate of 0.036-0.072 mg/(cm^2*day) in the present study with literature data and found it to be 28-56 times slower than the *in vitro* measured average corrosion rate for different metallic alloys (2.016 mg/[cm^2*day])[34] and similar to the slowest corrosion rates among 31 different uncoated Mg-alloys tested by Kirkland et al[35].

Because of their advantages, bioresorbable scaffolds are heralded as the fourth revolution in interventional cardiology[1]. The best-performing AMS-3.0 version, 85/15H, is already under clinical investigation within the BIOSOLVE-I study[36] (ClinicalTrials.gov: NCT01168830). Apart from the research on Mg- or iron-based bioresorbable metallic scaffold platforms[1,8,37], encouraging results have been obtained with bioresorbable poly(L-lactide) scaffolds coated with poly(D,L-lactide)-eluting everolimus[38,39].

STUDY LIMITATIONS

In a study comparing bioresorbable scaffolds and permanent stents, it was not possible to blind the QCA analyst, the histomorphology operator, and the study pathologist to device characteristics. Besides, the choice of morphometry parameters was limited to the intimal area and medial area, while vessel luminal area, the area within the internal elastic lamina, the area within the external elastic lamina, and the percent area stenosis were not used as they may be influenced by potential vessel shrinkage after euthanasia in conditions when there is no permanent stent to prevent this *post mortem* artefact.

One of the major limitations of the drug-free AMS-1 scaffolds, the constrictive vascular remodelling[17], may be rectified in part by paclitaxel elution, as observed in the aforementioned BIOSOLVE-I study[36]. Regrettably, the potentially insightful intravascular ultrasound evaluation of this issue was not performed within the present study. Of note, the drug release kinetics for AMS-3.0 scaffolds at later time points (>60-90 days) is probably quicker *in vivo* than that seen *in vitro* **(Figure 7)** because of scaffold fragmentation and polymer absorption *in vivo*.

The applied healthy porcine coronary model cannot fully reflect a diseased human coronary artery. The ability to transfer these animal data to humans is limited by the missing simulation of the potential effects of a pre-established neointimal hyperplasia or atherosclerotic disease. Besides, there may be a distinct species response to the antiproliferative and immunosuppressive effects of stents. Nevertheless, animal models provide mechanistic insight into fundamental biological processes and appear to indicate relative safety[28], even if incapable of replicating fully the clinical outcomes such as late stent thrombosis, myocardial infarction, and death. With respect to the choice of TAXUS Liberté as a main control stent, it has been widely used clinically but may no longer be considered as the gold standard in view of late stent thrombosis[40-43].

To confine the size of the study, our comparison did not involve AMS-3.0 scaffolds without antiproliferative drug or without PLGA, which prevented an assessment of the individual impact of these components.

Conclusion

By selecting suitable paclitaxel-elution kinetics, it was feasible to develop a bioresorbable magnesium scaffold whose efficacy and healing characteristics in a porcine coronary model are comparable with those of established paclitaxel-eluting permanent metallic stents.

ACKNOWLEDGEMENTS

The study was funded by Biotronik AG (Bülach, Switzerland). The authors would like to thank Dejan Danilovic, PhD, for assistance in the medical writing, and Nico Bruining, PhD, for critical reading and constructive discussion of the manuscript.

Conflict of interest statement

E. Wittchow, N. Adden, J. Riedmüller and M. Braune are employees of Biotronik SE & Co. KG. C. Savard is an employee of AccelLAB Inc. R. Waksman receives grant research support and consulting fees from Biotronik.

References

1. Onuma Y, Serruys PW. Bioresorbable scaffold: the advent of a new era in percutaneous coronary and peripheral revascularization? *Circulation.* 2011;123:779-97.

2. Serruys PW, Garcia-Garcia HM, Onuma Y. From metallic cages to transient bioresorbable scaffolds: change in paradigm of coronary revascularization in the upcoming decade? *Eur Heart J.* 2012;33:16-25.

3. Wykrzykowska JJ, Onuma Y, Serruys PW. Advances in stent drug delivery: the future is in bioabsorbable stents. *Expert Opin Drug Deliv.* 2009;6:113-26.

4. Heublein B, Rohde R, Kaese V, Niemeyer M, Hartung W, Haverich A. Biocorrosion of magnesium alloys: a new principle in cardiovascular implant technology? *Heart.* 2003;89:651-6.

5. Waksman R, Pakala R, Kuchulakanti PK, Baffour R, Hellinga D, Seabron R, Tio FO, Wittchow E, Hartwig S, Harder C, Rohde R, Heublein B, Andreae A, Waldmann KH, Haverich A. Safety and efficacy of bioabsorbable magnesium alloy stents in porcine coronary arteries. *Catheter Cardiovasc Interv.* 2006;68:607-17.

6. Erne P, Schier M, Resink TJ. The road to bioabsorbable stents: reaching clinical reality? *Cardiovasc Intervent Radiol.* 2006;29:11-6.

7. Erbel R, Di Mario C, Bartunek J, Bonnier J, de Bruyne B, Eberli FR, Erne P, Haude M, Heublein B, Horrigan M, Ilsley C, Bose D, Koolen J, Luscher TF, Weissman N, Waksman R. Temporary scaffolding of coronary arteries with bioabsorbable magnesium stents: a prospective, non-randomised multicentre trial. *Lancet.* 2007;369:1869-75.

8. Mani G, Feldman MD, Patel D, Agrawal CM. Coronary stents: a materials perspective. *Biomaterials.* 2007;28:1689-710.

9. Bosiers M, Deloose K, Verbist J, Peeters P. First clinical application of absorbable metal stents in the treatment of critical

limb ischemia: 12-month results. *Vascular Disease Management.* 2005;2:86-91.

10. Zartner P, Cesnjevar R, Singer H, Weyand M. First successful implantation of a biodegradable metal stent into the left pulmonary artery of a preterm baby. *Catheter Cardiovasc Interv.* 2005;66:590-4.

11. Böse D, Eggebrecht H, Erbel R. Absorbable metal stent in human coronary arteries: imaging with intravascular ultrasound. *Heart.* 2006;92:892.

12. Barlis P, Tanigawa J, Di Mario C. Coronary bioabsorbable magnesium stent: 15-month intravascular ultrasound and optical coherence tomography findings. *Eur Heart J.* 2007;28:2319.

13. Ghimire G, Spiro J, Kharbanda R, Roughton M, Barlis P, Mason M, Ilsley C, Di Mario C, Erbel R, Waksman R, Dalby M. Initial evidence for the return of coronary vasoreactivity following the absorption of bioabsorbable magnesium alloy coronary stents. *EuroIntervention.* 2009;4:481-4.

14. Bosiers M, Peeters P, D'Archambeau O, Hendriks J, Pilger E, Duber C, Zeller T, Gussmann A, Lohle PN, Minar E, Scheinert D, Hausegger K, Schulte KL, Verbist J, Deloose K, Lammer J. AMS INSIGHT- absorbable metal stent implantation for treatment of below-the-knee critical limb ischemia: 6-month analysis. *Cardiovasc Intervent Radiol.* 2009;32:424-35.

15. Waksman R, Erbel R, Di Mario C, Bartunek J, de Bruyne B, Eberli FR, Erne P, Haude M, Horrigan M, Ilsley C, Bose D, Bonnier H, Koolen J, Luscher TF, Weissman NJ. Early- and long-term intravascular ultrasound and angiographic findings after bioabsorbable magnesium stent implantation in human coronary arteries. *JACC Cardiovasc Interv.* 2009;2:312-20.

16. McMahon CJ, Oslizlok P, Walsh KP. Early restenosis following biodegradable stent implantation in an aortopulmonary collateral of a patient with pulmonary atresia and hypoplastic pulmonary arteries. *Catheter Cardiovasc Interv.* 2007;69:735-8.

17. Maeng M, Jensen LO, Falk E, Andersen HR, Thuesen L. Negative vascular remodelling after implantation of bioabsorbable magnesium alloy stents in porcine coronary arteries: a randomised comparison with bare-metal and sirolimus-eluting stents. *Heart.* 2009;95:241-6.

18. Jabara R, Chronos N, Conway D, Molema W, Robinson K. Evaluation of a novel slow-release paclitaxel-eluting stent with a bioabsorbable polymeric surface coating. *JACC Cardiovasc Interv.* 2008;1:81-7.

19. Grube E, Silber S, Hauptmann KE, Mueller R, Buellesfeld L, Gerckens U, Russell ME. TAXUS I: six- and twelve-month results from a randomized, double-blind trial on a slow-release paclitaxel-eluting stent for de novo coronary lesions. *Circulation.* 2003;107:38-42.

20. Kamath KR, Barry JJ, Miller KM. The Taxus drug-eluting stent: a new paradigm in controlled drug delivery. *Adv Drug Deliv Rev.* 2006;58:412-36.

21. Silber S. Cypher versus taxus: are there differences? *J Interv Cardiol.* 2005;18:441-6.

22. Miyajima M, Koshika A, Okada J, Ikeda M. Effect of polymer/basic drug interactions on the two-stage diffusion-controlled release from a poly(L-lactic acid) matrix. *J Control Release.* 1999;61:295-304.

23. Rodriguez AE, Vigo CF, Delacasa A, Mieres J, Fernandez-Pereira C, Bernardi V, Bettinoti M, Rodriguez-Granillo AM, Rodriguez-Granillo G, Santaera O, Curotto V, Rubilar B, Tronge J, Palacios IF, Antoniucci D. Efficacy and safety of a double-coated paclitaxel-eluting coronary stent: the EUCATAX trial. *Catheter Cardiovasc Interv.* 2011;77:335-42.

24. Pache J, Kastrati A, Mehilli J, Schuhlen H, Dotzer F, Hausleiter J, Fleckenstein M, Neumann FJ, Sattelberger U, Schmitt C, Muller M, Dirschinger J, Schömig A. Intracoronary stenting and angiographic results: strut thickness effect on restenosis outcome (ISAR-STEREO-2) trial. *J Am Coll Cardiol.* 2003;41:1283-8.

25. Tung R, Kaul S, Diamond GA, Shah PK. Narrative review: drug-eluting stents for the management of restenosis: a critical appraisal of the evidence. *Ann Intern Med.* 2006;144:913-9.

26. Jimenez JM, Davies PF. Hemodynamically driven stent strut design. *Ann Biomed Eng.* 2009;37:1483-94.

27. Perez G, Rodriguez-Granillo AM, Mieres J, Llaurado C, Rubilar B, Risau G, Fernandez-Pereira C, Rodriguez AE. New coating stent design for patients with high-risk coronary lesions for thrombotic events: early and long-term results of the Camouflage registry. *J Invasive Cardiol.* 2009;21:378-82.

28. Schwartz RS, Edelman E, Virmani R, Carter A, Granada JF, Kaluza GL, Chronos NA, Robinson KA, Waksman R, Weinberger J, Wilson GJ, Wilensky RL. Drug-eluting stents in preclinical studies: updated consensus recommendations for preclinical evaluation. *Circ Cardiovasc Interv.* 2008;1:143-53.

29. Carter AJ, Aggarwal M, Kopia GA, Tio F, Tsao PS, Kolata R, Yeung AC, Llanos G, Dooley J, Falotico R. Long-term effects of polymer-based, slow-release, sirolimus-eluting stents in a porcine coronary model. *Cardiovasc Res.* 2004;63:617-24.

30. Nakazawa G, Finn AV, John MC, Kolodgie FD, Virmani R. The significance of preclinical evaluation of sirolimus-, paclitaxel-, and zotarolimus-eluting stents. *Am J Cardiol.* 2007;100:36M-44M.

31. Turco MA, Ormiston JA, Popma JJ, Mandinov L, O'Shaughnessy CD, Mann T, McGarry TF, Wu CJ, Chan C, Webster MW, Hall JJ, Mishkel GJ, Cannon LA, Baim DS, Koglin J. Polymer-based, paclitaxel-eluting TAXUS Liberte stent in de novo lesions: the pivotal TAXUS ATLAS trial. *J Am Coll Cardiol.* 2007;49:1676-83.

32. Ali SA, Doherty PJ, Williams DF. Molecular biointeractions of biomedical polymers with extracellular exudate and inflammatory cells and their effects on the biocompatibility, in vivo. *Biomaterials*. 1994;15:779-85.

33. Witte F, Fischer J, Nellesen J, Crostack HA, Kaese V, Pisch A, Beckmann F, Windhagen H. In vitro and in vivo corrosion measurements of magnesium alloys. *Biomaterials.* 2006;27:1013-8.

34. Grogan JA, O'Brien BJ, Leen SB, McHugh PE. A corrosion model for bioabsorbable metallic stents. *Acta Biomater.* 2011;7:3523-33.

35. Kirkland NT, Lespagnol J, Birbilis N, Staiger MP. A survey of bio-corrosion rates of magnesium alloys. *Corrosion Science.* 2010;52:287-91.

36. Haude M, Erbel R, Erne P, Verheye S, Degen H, Böse D, Vermeersch P, Wijnbergen I, Weissman N, Prati F, Waksman R, Koolen J. Safety and performance of the drug-eluting absorbable metal scaffold (DREAMS) in patients with de-novo coronary lesions: 12 month results of the prospective, multicentre, first-in-man BIOSOLVE-I trial. *Lancet.* 2013 Jan 14. [Epub ahead of print]

37. Moravej M, Mantovani D. Biodegradable metals for cardiovascular stent application: interests and new opportunities. *Int J Mol Sci.* 2011;12:4250-70.

38. Onuma Y, Serruys PW, Perkins LE, Okamura T, Gonzalo N, Garcia-Garcia HM, Regar E, Kamberi M, Powers JC, Rapoza R, van Beusekom H, van der Giessen W, Virmani R. Intracoronary optical coherence tomography and histology at 1 month and 2, 3, and 4 years after implantation of everolimus-eluting bioresorbable vascular scaffolds in a porcine coronary artery model: an attempt to decipher the human optical coherence tomography images in the ABSORB trial. *Circulation.* 2010;122:2288-300.

39. Serruys PW, Ormiston JA, Onuma Y, Regar E, Gonzalo N, Garcia-Garcia HM, Nieman K, Bruining N, Dorange C, Miquel-Hebert K, Veldhof S, Webster M, Thuesen L, Dudek D. A bioabsorbable everolimus-eluting coronary stent system (ABSORB): 2-year outcomes and results from multiple imaging methods. *Lancet.* 2009;373:897-910.

40. Wenaweser P, Daemen J, Zwahlen M, van Domburg R, Juni P, Vaina S, Hellige G, Tsuchida K, Morger C, Boersma E, Kukreja N, Meier B, Serruys PW, Windecker S. Incidence and correlates of drug-eluting stent thrombosis in routine clinical practice. 4-year results from a large 2-institutional cohort study. *J Am Coll Cardiol.* 2008;52:1134-40.

41. Jensen LO, Tilsted HH, Thayssen P, Kaltoft A, Maeng M, Lassen JF, Hansen KN, Madsen M, Ravkilde J, Johnsen SP, Sorensen HT, Thuesen L. Paclitaxel and sirolimus eluting stents versus bare metal stents: long-term risk of stent thrombosis and other outcomes. From the Western Denmark Heart Registry. *EuroIntervention.* 2010;5:898-905.

42. Smits PC, Kedhi E, Royaards KJ, Joesoef KS, Wassing J, Rademaker-Havinga TA, McFadden E. 2-year follow-up of a randomized controlled trial of everolimus- and paclitaxel-eluting stents for coronary revascularization in daily practice. COMPARE (Comparison of the everolimus eluting XIENCE-V stent with the paclitaxel eluting TAXUS LIBERTE stent in all-comers: a randomized open label trial). *J Am Coll Cardiol.* 2011;58:11-8.

43. Räber L, Magro M, Stefanini GG, Kalesan B, van Domburg RT, Onuma Y, Wenaweser P, Daemen J, Meier B, Juni P, Serruys PW, Windecker S. Very late coronary stent thrombosis of a newer-generation everolimus-eluting stent compared with early-generation drug-eluting stents: a prospective cohort study. *Circulation.* 2012;125:1110-21.